

# Acoustic emission in asphalt mixtures at low temperature

X. Li, M. O. Marasteanu & J. F. Labuz

*Department of Civil Engineering, University of Minnesota, Minneapolis, USA*

**ABSTRACT:** The objective of the research was to investigate the use of acoustic emission to analyze the microstructural phenomena of damage and the corresponding macroscopic behavior in asphalt mixtures tested at low temperature. An acoustic emission system with eight channels of recording was used to monitor the specimens tested in creep and in strength testing. The source location and the AE event count were used to illustrate the relationship between the micro damage and macroscopic behavior for the two different test conditions. The analysis indicates that a damage zone develops in both the creep and the strength tests. The damage zone changes with the test temperature and the loading level applied during the creep test.

## 1 INTRODUCTION

It is well recognized that asphalt mixtures have complex temperature-sensitive behaviors. The response to a given loading is strongly dependent on temperature and loading path. A change of a few degrees in temperature induces dramatic changes in behavior of the asphalt mixture. The behavior can vary from relatively ductile at higher temperature to brittle at lower temperature.

Low temperature cracking is the most significant distresses in asphalt pavements built in areas with cold climates. Low temperature cracking is attributed to tensile stresses induced in the asphalt pavement as the temperature drops to extremely low values. The accumulation of tensile stress to a certain level is associated with the formation of microcracks, which release energy in the form of elastic waves called acoustic emission (AE). The current AASHTO specification for asphalt mixture low temperature characterization consists of two tests: the indirect tensile creep test (ITC) and the indirect tensile strength test (ITS). For both tests, cylindrical specimens of 150 mm diameter x 50 mm thickness are loaded in compression across the diametral plane.

This paper investigates the use of AE to analyze the microstructural phenomena and the corresponding macroscopic behavior in asphalt mixtures tested at three low temperatures. For each test temperature, two different loading levels were used in the creep test and one constant stroke rate of 1 mm/min was employed in the strength tests. This was done to identify the damage development with loading levels

and to compare the damage zone in creep and failure tests.

## 2 BACKGROUND

AE methods represent a well-documented and widely used tool to characterize microscopic fracture processes and therefore to evaluate damage growth in brittle materials. An acoustic emission is defined as a transient elastic wave generated by the sudden release of energy from localized damage processes within the stressed material. This energy release causes the propagation of stress waves that can be detected at the surface of the material. Acoustic emissions result from microcracking, dislocation movement, phase transformation, and other irreversible changes in the material.

Due to its capability of detecting internal damage, AE has been used for many years to study the behavior of materials such as rock and concrete. By studying the occurrence of AE events, the investigations are generally focused on the cumulative number of AE events, the rate of occurrence, amplitude distribution, energy and frequency distribution.

Compared to the vast number of studies performed on Portland cement concrete and rocks, a literature search on the use of AE in asphalt materials results in a very limited number of references. This is due to the fact that for most service temperatures asphalt mixtures display viscous and ductile behavior and the development of defects is gradual and does not produce emissions that can be detected.

In one of the first efforts to document the use of AE to characterize the fracture of asphalt mixtures

under thermal loading conditions at low temperatures, Valkering & Jongeneel (1991) used a single piezoelectric transducer mounted on the surface of the specimen. The cumulative event counting was analyzed to determine how damage accumulates during loading. Their work was followed by a small number of studies performed by different authors who also limited their analyses to counting of AE events.

AE techniques were also investigated during the Strategic Highway Research Program (SHRP) in an effort to better characterize the cohesive, adhesive and thermal properties of asphalt binders (Chang, 1994; Wang, 1995; Qin, 1995). However, this work was performed at higher temperatures that considerably limited the analysis of the AE results. Sinha (1998) reported on the AE activity in unrestrained asphalt mixture samples exposed to thermal cycling at low temperatures to show that micro cracking occurs in asphalt mixtures due to the difference between the thermal contraction coefficients of the aggregate and of the asphalt binder. Hesp et al. (2001) investigated AE activity in restrained asphalt mixture samples undergoing various temperature cycles and Cordel et al. (2003) used two transducers to detect the AE events in asphalt mixture direct tension tests performed at low temperatures.

In a recent study by Li & Marasteanu (2006), the accumulated AE events obtained from an AE system with eight channels of recording were analyzed to illustrate the relationship between the micro damage and macroscopic behavior of the asphalt mixtures at different loading levels. In addition, the initiation and propagation of the cracking were observed using the localization of the event source and the fracture process zone in the asphalt mixtures was measured by observing the distribution of microcracks with different energy levels.

### 3 EXPERIMENTAL PROCEDURE

The asphalt mixture used in this study was prepared using the Superpave design procedure outlined in SP-2. One asphalt binder with performance grade (PG) 58-34 and modified by styrene-butadiene-styrene (SBS) was used. Granite aggregate was selected to prepare the mixture. Cylindrical specimens 150 mm by 170 mm were compacted using the Brovold gyratory compactor. A 4% target air voids was achieved after compaction. The compacted samples were then cut into 3 slices with 50 mm in thickness.

The indirect tensile test set-up is shown in Figure 1. A sample with dimensions of 150 mm diameter by 50 mm height was loaded in static compression across its diametral plane. Different load levels were applied in the creep test to investigate the effect of load levels on the development of the micro damage during the creep test. A constant loading rate of 10

kN/s was used at the beginning of the creep test. Following the creep test, an indirect tensile strength test was performed at the same temperature. A constant stroke rate of 1 mm/min was applied during the strength test until failure.

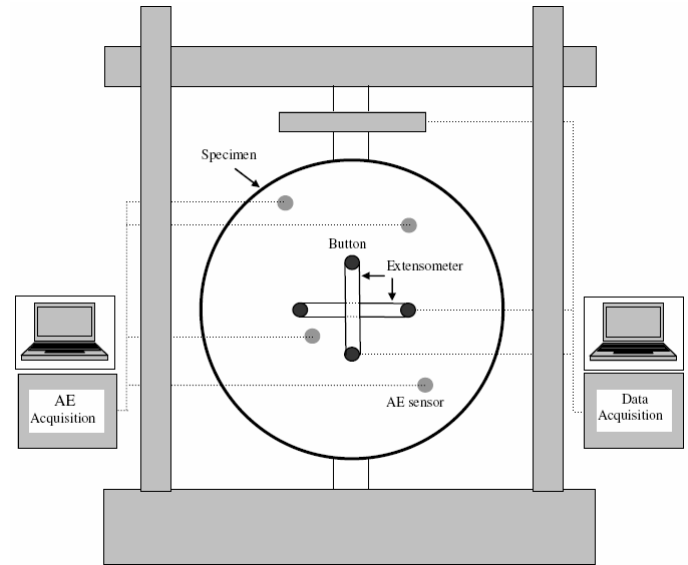


Figure 1. Schematic of Experimental Setup.

An AE system with eight channels of recording was used to monitor the asphalt mixture specimens tested in creep and strength tests. The AE event signals were recorded using four DAQ cards (Model PCI-5112, National Instruments). Each card had two independent channels which acquired AE signals detected by eight piezoelectric sensors (Model S9225, Physical Acoustics Corporation). Four sensors were mounted on each side of the specimen using M-Bond 200, a modified alkyl cyanoacrylate. The preamplification of the AE signals was provided by eight preamplifiers (Model 1220C, PAC) with a gain set to 40 dB. One of the sensors was used as a trigger, which was often the one closest to the tip of the initial notch. Trigger level was set at 10 mV in this research. Once the recording was triggered, signals were band-pass filtered (0.1-1.2 MHz) and sampled at 20 MHz over 200 microseconds. Considering the ringing of the resonant sensor, a sleep time of 9 milliseconds between two consecutive events was prescribed during which the system could not be triggered. The velocity of propagation of the longitudinal waves was determined by generating an elastic wave by pencil lead (0.5 mm diameter) breakage on the opposite side of the specimens.

Tests were performed in a MTS servo-hydraulic testing system. The TestStar IIs control system was used to set up and perform the tests and to collect the data. The software package MultiPurpose TestWare was used to custom-design the tests and collect the data. All tests were performed inside an environmental chamber. Liquid nitrogen tanks were used to obtain the required low temperature. The temperature was controlled by MTS temperature

controller and verified using an independent platinum RTD thermometer.

Three test temperatures,  $-12\text{ }^{\circ}\text{C}$ ,  $-24\text{ }^{\circ}\text{C}$  and  $-36\text{ }^{\circ}\text{C}$  were selected based on the PG lower limit of the asphalt binder. Two specimens, one replicate for two different loading levels, were fabricated for the creep testing at each temperature. The specimen used for the creep test at the lower loading level was also used for the strength test, 30 minutes after the creep test.

## 4 DISCUSSION OF RESULTS

The mechanical response for all three temperatures during the strength tests are shown in Figure 2. At the highest temperature ( $-12\text{ }^{\circ}\text{C}$ ), the asphalt mixture is more ductile and it has lower peak load and larger displacements. At the lowest temperature ( $-36\text{ }^{\circ}\text{C}$ ), the material is brittle. At  $-24\text{ }^{\circ}\text{C}$  temperature, the mixture exhibits an intermediate behavior.

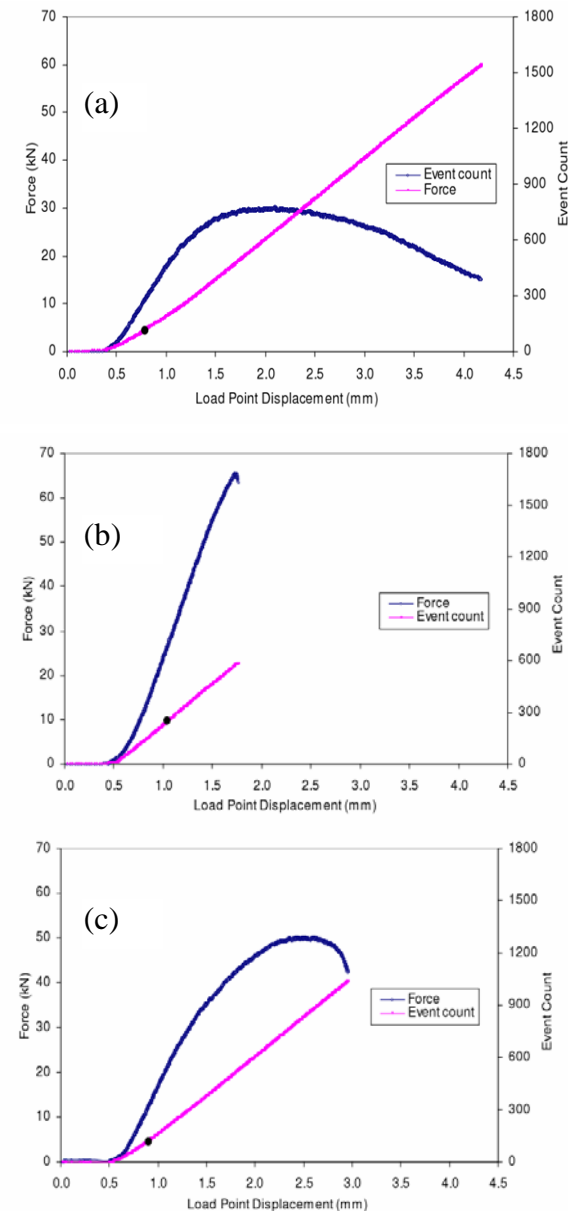


Figure 2. Load and AE count versus displacement from strength test: (a)  $-12\text{ }^{\circ}\text{C}$ ; (b)  $-24\text{ }^{\circ}\text{C}$ ; (c)  $-36\text{ }^{\circ}\text{C}$ .

### 4.1 AE event count

The event count curves under different temperatures follow a similar pattern. Very few AE events were detected at the beginning of the test but soon after the AE rate was constant at 7 to 8 events per second. The black circle on the event count curve shows the loading level in the creep test performed before the strength test. For all strength plots under different temperatures, more than 100 events were recorded before the loading level applied in the creep test was reached. This appears to indicate that the Kaiser effect, which describes the phenomenon that a material under load emits acoustic waves only after a primary load level is exceeded, is not applicable to the material investigated in this study.

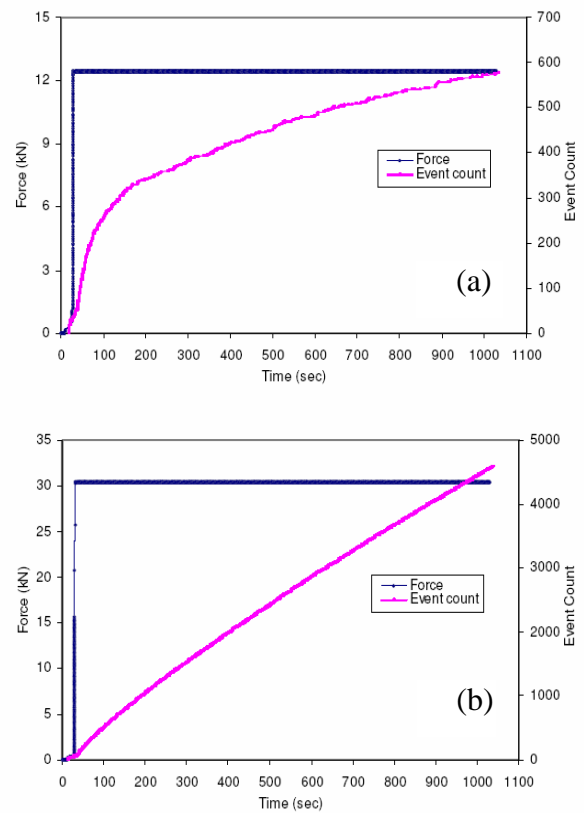


Figure 3. Typical plot for load and AE count versus time from creep test: (a) 12.5 kN at  $-24\text{ }^{\circ}\text{C}$ ; (b) 30 kN at  $-24\text{ }^{\circ}\text{C}$ .

A typical plot of loading and AE event count versus time for the creep test is shown in Figure 3. The two creep tests with different load level under the same temperature show a similar trend with time. AE events were recorded with a fast event rate immediately after the creep load level was applied in a short time and the event rate decreased with time. It was found that more events were recorded in the creep test with higher loading level.

### 4.2 AE source location

The source location of the AE events can be inferred by investigating the differences of the first time of

arrival among the transducers placed at different locations on the specimen. Therefore, it is necessary to determine the arrival time of the elastic waves for each sensor from the recorded AE event. The correct picking of the first arrival strongly affects the accuracy of the source location (Labuz et al., 1997). The mean amplitude and standard deviation of the noise during the pre-trigger period was calculated and a threshold was set at three times the standard deviation from the mean. By measuring the time at which the signal passes this threshold value for each sensor, the relative arrival time can be obtained.

Once the arrival times of the event were determined from the sensor records, the location of the AE event source can be estimated. It should be noted that not all events can be located. It was found that only 143 events were located with 10 mm error for the creep test under the lower loading level at  $-24\text{ }^{\circ}\text{C}$ . Therefore, event locations with 143 events are selected and plotted for the comparison. A rectangle was drawn to contain 90% of these 143 events. Figure 4 shows the first 143 AE locations obtained from the strength test under different temperatures. It is found that the size of the damage zone, which is defined here as the area with microcracking inside the rectangle, changes with temperature for the strength test. The width of this zone decreases with the decrease in test temperature. While no clear difference is found for the length of the damage zone for the two higher temperatures, the damage zone at the lowest temperature is obviously longer than the damage zones at the two higher temperatures.

Figures 5, 6 and 7 show the locations for the last 143 events during the creep test for all temperatures. It is observed that for all temperatures the damage zone obtained at the higher load was significantly larger in width than the zone obtained from the lower load creep test. For example, the damage zone obtained from the lower load level creep test at  $-12\text{ }^{\circ}\text{C}$  is 24 mm in width, while the damage zone from the higher load level creep at the same temperature is 29 mm wide. For the creep tests with relatively lower load level, both the width and length of the damage zone decreased with the decrease of test temperature (Figs 5a, 6a, 7a). For example, the damage zone obtained from the lower load level creep at  $-24\text{ }^{\circ}\text{C}$  is 21 mm by 60 mm, while the size of damage zone from the higher load level creep at  $-36\text{ }^{\circ}\text{C}$  is 18 mm by 55 mm.

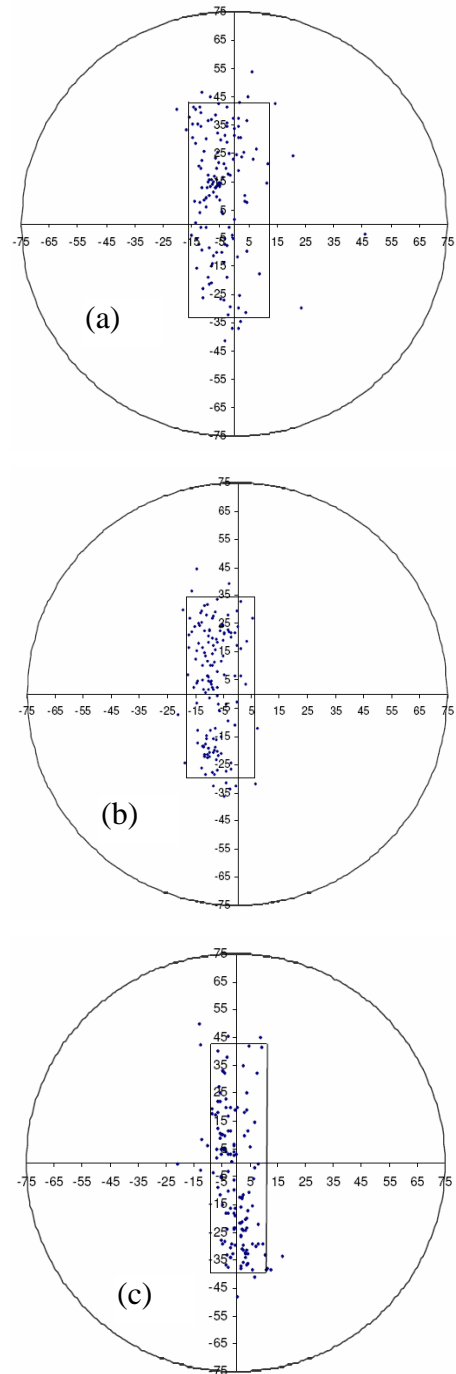


Figure 4. Event locations and damage zone for strength test: (a)  $-12\text{ }^{\circ}\text{C}$ ; (b)  $-24\text{ }^{\circ}\text{C}$ ; (c)  $-36\text{ }^{\circ}\text{C}$ .

The comparison for the damage zone obtained from both creep test and strength test shows that for all temperatures the size of damage zone obtained from strength test is very close to the size of damage zone from the creep test with higher loading level, which was approximately equal to 50% to 60% of the strength value (Figs 5b, 6b, 6c).

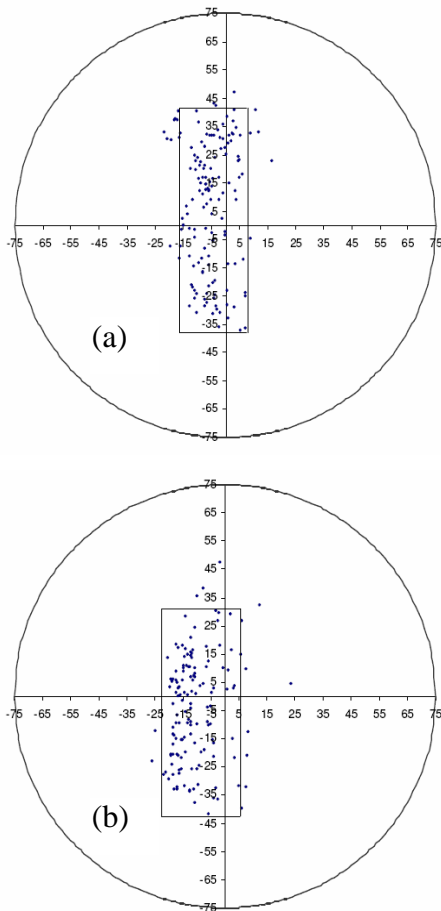


Figure 5. Event locations and damage zone for creep test at -12°C: (a) 10 kN (33% of strength); (b) 15 kN (50% of strength)

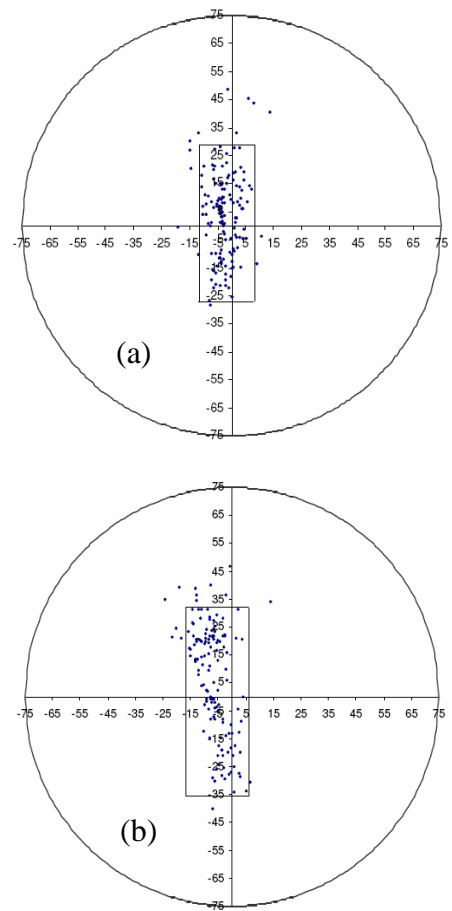


Figure 7. Event locations and damage zone for creep test at -36°C: (a) 25 kN (38% of strength); (b) 40 kN (61% of strength)

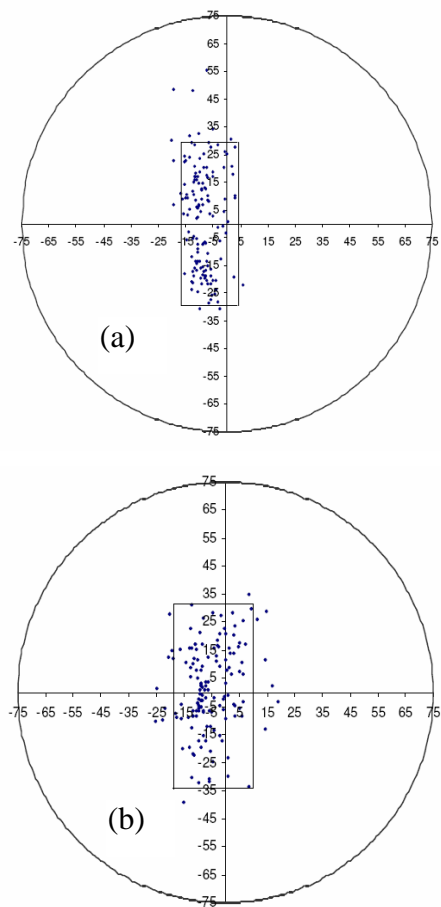


Figure 6. Event locations and damage zone for creep test at -24°C: (a) 12.5 kN (25% of strength); (b) 30 kN (60% of strength).

## 5 CONCLUSION

Indirect tensile creep tests with two different loading levels, and strength tests were performed under three different test temperatures for one asphalt mixture. An acoustic emission system with eight channels of recording was used to monitor the development of microcracking in the specimens for both tests.

The experimental data show that the asphalt mixture presented more brittle behavior with decrease in test temperature. Few events were recorded at the beginning of the strength test but the AE rate was constant at 7 to 8 events per second after certain loading level. A similar event rate was found immediately after the creep load was applied, but the event rate decreased with time. Creep tests at higher load levels were found to produce more events than the tests with lower load levels for all test temperatures. The Kaiser effect was not applicable for the tested specimens.

It was observed that the width of the damage zone developed during strength tests decreased with the decrease of temperature and the damage zone obtained from the higher loading level creep test was significantly larger in width than the zone obtained from the lower loading level creep test. The size of

the damage zone was found to decrease with temperature decrease for the creep tests. The damage zone obtained from strength test was approximately equal to that from creep test with a load level about 50% to 60% of the strength value.

## REFERENCES

- Chang W. V. 1994. Application of Acoustic Emission to Study the Cohesive and Adhesive Strength of Asphalt. Strategic Highway Research Program, SHRP-A-682, pp. 81-148.
- Cordel S., Benedetto H.Di., Malot M., Chaverot P., and Perraton D.2003. Fissuration à basse température des enrobés bitumineux -essai de retrait thermique empêché et émission acoustique. 6th International RILEM Symposium, Performance Testing & Evaluation of Bituminous Materials (PTEB 03), Editor Partl, M., pp. 465-472, Zurich, 2003.
- Hesp S. A. M., Smith B. J. 2001. The Effect of Filler Particle Size on Low and High Temperature Performance of Asphalt Mastics and Mixtures. Journal of the Association of Asphalt Paving Technologists, Vol. 70, pp. 492-542.
- Labuz J. F., Dai S-T., and Shah K. R. 1997. Identifying Failure Through Location of Acoustic Emission. Transportation Research Record 1526, TRB, National Research Council, Washington, D.C., pp.104-111.
- Li X., and Marasteanu M.O. 2006. Investigation of Low Temperature Cracking in Asphalt Mixtures by Acoustic Emission. International Journal of Road Material and Pavement Design, Vol. 7-No. 4/2006, pp.491-512.
- Qin X.1995. Adhesion properties of polymeric materials. Ph.D. thesis, University of Southern California, Chemical Engineering.
- Sinha N. K. 1998. Acoustic emission in asphalt subjected to thermal cycling at low temperature. In Acoustic emission/microseismic activity in geologic structures and materials, Proceedings of the Six Conference, by Reginald Hardy, Jr., H., Pennsylvania State University, Vol. 21, 109-120.
- Valkering C. P., and Jongeneel D.J. (1991). Acoustic emission for evaluating the relative performance of asphalt mixes under thermal loading conditions. Journal of the Association of Asphalt Paving Technologists, vol. 60, 160-187.
- Wang H.-C. 1995. Ultrasonic and acoustic emission in nondestructive evaluation of viscoelastic solids – elastomer, human cornea and asphalt. Ph.D. thesis, University of Southern California, Chemical Engineering.